Elimination of Two Level Fluctuators in Superconducting Quantum Bits by an Epitaxial Tunnel Barrier

Seongshik Oh,[1,2] Katarina Cicak,[1] Jeffrey S. Kline,[1] Mika A. Sillanpää,[1] Kevin D. Osborn,[1] Jed D. Whittaker,[1] Raymond W. Simmonds[1] and David P. Pappas[1]

[1]National Institute of Standards and Technology, Boulder, Colorado 80305, USA

[2]Department of Physics, University of Illinois, Urbana, Illinois 61801, USA

Quantum computing based on Josephson junction technology is considered promising due to its scalable architecture. However, decoherence is a major obstacle. Here, we report the first evidence for improved Josephson quantum bits (qubits) using a new material, a single-crystal Al_2O_3 tunnel barrier. We have found an ~80% reduction in the density of the spectral splittings that indicate the existence of two-level fluctators (TLFs) in amorphous tunnel barriers. The residual ~20% TLFs can be attributed to interfacial effects that may be further reduced by different electrode materials. These results show that decoherence sources in the tunnel barrier of Josephson qubits can be identified and eliminated.

Scalable superconducting circuits based on Josephson junctions are a promising approach to quantum computing.[1] These circuits allow for the design and manipulation of "artificial atoms" that act as individual quantum bits (qubits). In these types of systems, single-qubit quantum oscillations,[2-6] entanglement of two qubits,[7-10] a quantum gate operation,[11] and coupling between a qubit and a quantum harmonic oscillator[12,13] have already been demonstrated. However, one of the biggest obstacles to building a quantum computer is decoherence, which destroys quantum information and can remove energy from the system. Unlike other qubit implementations such as NMR[14] and trapped ions,[15] the Josephson qubit is more strongly coupled to its environment making it more susceptible to uncontrolled decoherence sources. For example, coupling to the outside world occurs through the electrical leads and to the device-level surroundings through direct electromagnetic interactions. Decoherence can be suppressed by means of filtering and shielding techniques.[16] At the device level, progress has been made by optimizing the circuit design,[17] operating the qubit at an optimal bias point,[3] or using special measurement techniques such as a spin-echo pulse configuration.[6,18] However, such approaches may not be effective when decoherence sources originate within material components forming the qubit.

According to a series of recent reports,[19-21] it is now clear that the coherence of Josephson qubits fabricated with amorphous aluminum oxide (AlO_x) tunnel barriers is destroyed by spectral splittings that indicate the existence of two-level fluctuators (TLFs) in the tunnel barrier.[21-25] The qubit's coherence is disrupted by quantum states of the TLFs that interact with the qubit. This interaction manifests itself as forbidden regions

(splittings) in the energy spectrum of the qubit. Operation of the qubit at these forbidden regions distorts and suppresses coherent quantum oscillations of the qubit state.[19] Even when operated away from these regions, qubits show reduced measurement fidelity[20] and energy relaxation times (T_1).[21] TLFs may also be responsible for ubiquitous low-frequency $1/f$ noise that appears to shorten the qubit dephasing time (T_2).[24-27]

It has been speculated that the amorphous nature of AlO_x tunnel barrier, the prevalent barrier type used in most Josephson junction devices including qubits, is responsible for these splittings[19,21,25] and that a single-crystal (e.g., Al_2O_3) barrier may solve this problem. Since amorphous AlO_x tunnel barriers were introduced more than four decades ago,[28] they have been widely used in superconducting as well as room temperature devices. Efforts to fabricate devices using crystalline Al_2O_3 barriers resulted only in low quality Josephson junctions.[29] To date, research on superconducting Josephson junctions has not revealed a clear understanding of how tunnel barrier crystallinity affects the density of TLFs within tunnel barriers and the barrier tunnelling properties. Recently, however, we successfully fabricated the first high quality Josephson junctions using a single-crystal, epitaxial Al_2O_3 tunnel barrier.[30] Here, we report the successful integration of these single-crystal, epitaxial Al_2O_3 tunnel barriers into Josephson phase qubits and present the first measurements showing a correlation between the crystallinity of the tunnel barrier and density of TLFs in the qubit.

The qubit devices were fabricated from a trilayer grown in ultra-high vacuum (UHV). The trilayers were grown on a single-crystal Al_2O_3 (0001) substrate. They are composed of an epitaxial base rhenium (Re) layer, the single crystal Al_2O_3 tunnel barrier, and a

polycrystalline top aluminum (Al) layer. Reflection high-energy electron diffraction (RHEED) was used to monitor the growth of all three layers. Characteristic streaks and rings were observed for the single-crystal and polycrystalline layers, respectively, as shown in Fig. 1.

This trilayer was then fabricated into several flux-biased phase qubits using conventional thin-film optical lithography techniques.[30] An optical image of one of the devices is shown in Fig. 2(a). The circuit design is identical to that of the previously studied $Al/AlO_x/Al$ qubits[20,21] with a qubit junction area of 70 μm^2. The cross-sectional view of the qubit is depicted in Fig. 2(b), where all the component layers are shown: the amorphous SiO_2 wiring insulator, the epitaxial Re base, the epitaxial Al_2O_3 tunnel barrier, the *in situ* evaporated top Al and the *ex situ* sputtered Al used for wiring connections. As shown in Fig. 2(a) and (c), the on-chip qubit circuitry is comprised of a flux-bias coil and a measurement DC-SQUID in addition to the qubit.

The qubit is represented by the two lowest energy states, denoted by $|0\rangle$ and $|1\rangle$, of the quantum phase across a single Josephson junction as described in more detail in Ref. 20. A metastable potential (energy) well is formed when the junction is current biased near its critical value, I_0. Both the energy spacing, $\hbar\omega_{10}$, between the two qubit states and the depth of the well are controlled by the bias current, I_ϕ, where an increase in I_ϕ toward I_0 decreases both the energy spacing and the well depth.

Spectroscopic measurements for the $|0\rangle \rightarrow |1\rangle$ transition frequency ω_{10} are shown in Fig. 3 as a function of bias current. The intensity of the color scale represents the probability for the qubit to be in its excited state, $|1\rangle$, after being irradiated by a long (~500 ns)

microwave pulse of amplitude $I_{\mu w}$ and frequency $\omega_{\mu w}$. Figure 3 compares the spectrum of an amorphous AlO_x barrier qubit (Fig. 3(a)) with an epitaxial Al_2O_3 barrier qubit (Fig. 3(b)) of the same design. While the amorphous barrier qubit shows many spectral splittings (i.e. TLFs), as previously reported,[19-21] the epitaxial barrier qubit shows fewer splittings over a similar frequency range. A more quantitative analysis shows that the amorphous barrier qubit has on average 24 splittings per 1 GHz bandwidth (measured on seven devices),[21] whereas the epitaxial one has on average 5 splittings over the same bandwidth (measured on three devices). The resolution of our measurement is 0.01 GHz. This shows that about ~80% of the splittings are eliminated in the epitaxial barrier qubit as compared to the amorphous barrier qubit.

The splittings observed in the qubit with amorphous AlO_x tunnel barriers are well understood by the TLF model of amorphous solids.[21,23-25] In an amorphous structure, ions are randomly located in metastable sites. When an ion tunnels between two nearby sites it naturally forms a TLF. The spectral splittings are a direct result of dipole coupling between the electric field across the Josephson tunnel barrier and the intrinsic dipole moments formed by displaced ions. This interaction can be described by an effective Hamiltonian,[21] $H_{\text{int}} = i(hS/2)(|1\rangle|g\rangle\langle 0|\langle e| - |0\rangle|e\rangle\langle 1|\langle g|)$, where $|0\rangle$ and $|1\rangle$ respectively represent the ground and the excited state of the qubit, while $|g\rangle$ and $|e\rangle$ represent the ground and the excited state of the TLF, and S corresponds to coupling strength or splitting size on resonance. This TLF model can also be used to explain the low temperature loss properties of both the amorphous AlO_x barrier and the amorphous wiring

SiO_2 insulator.[21] This model suggests that an ideal single-crystal tunnel barrier would not have any TLFs.

These data show that in our epitaxial qubit structure, there are still some residual TLFs. Two possible locations for these residual TLFs are: 1) in the bulk of the barrier or 2) at the interfaces between the barrier and the electrodes. We speculate that the most likely source is the interface between the Al_2O_3 tunnel barrier and the Al top electrode. First, this interface is not epitaxial. Second, interfacial oxygen ions can bond equally well with Al ions residing either in the electrode or the tunnel barrier. This situation is similar to the interface that exists in an amorphous AlO_x barrier qubit. Considering that the spacing between each layer of oxygen atoms within the tunnel barrier along the (0001) direction[31] of Al_2O_3 is 0.43 nm and the thickness of our tunnel barrier is ~1.5 nm, the amount of oxygen on the Al_2O_3-Al interface must be ~20-25 % of the total oxygen in the Al_2O_3 tunnel barrier. Therefore, even if the bulk of the single-crystal tunnel barrier is completely free of any TLFs, the Al_2O_3-Al interface can still contribute this percentage of the TLFs compared to amorphous AlO_x barrier qubits. This number is consistent with the observed density of residual TLFs. If this scenario is correct, an epitaxial barrier qubit with an epitaxial Re top electrode may show even fewer TLFs than the present qubit with an Al top electrode. An investigation of this hypothesis is currently underway.

The top inset of Fig. 3(b) shows a microwave driven oscillation (Rabi oscillation) of the epitaxial barrier qubit state measured at a bias point free of any splittings. Its energy decay time (~90 ns) is comparable to that of amorphous barrier qubits having the same SiO_2 wiring dielectric. This is consistent with the previous report[21] that decoherence at bias

points away from the splittings is dominated by the weakly-coupled TLFs residing in the wiring dielectric around the qubit, as shown in Fig. 2(b). The qubit performance may, therefore, be further improved if a less lossy wiring dielectric is utilized for the epitaxial qubit.

In summary, we have fabricated the first superconducting qubits with a single-crystal Al_2O_3 tunnel barrier. We have observed a substantial reduction in the density of TLFs compared to qubits with amorphous AlO_x barriers. Our result is the first demonstration that atomic engineering of the barrier crystallinity has made an observable improvement in the physical properties of tunnel barriers, in particular those used for superconducting qubits. This result also shows that qubits are a good test bed for studying TLFs in tunnel barriers. It may also give insights into the noise properties of a wide range of devices, from magnetic sensors to transistors, which are currently fabricated using amorphous insulators. Furthermore, improved Josephson junction technology could provide a significant impact on a variety of applications including microwave mixers, magnetometers, and bolometers.

This work is supported by ARO/DTO Quantum Information Science and Technology Program, by North Atlantic Treaty Organization (NATO), by National Research Council (NRC) and by National Institute of Standards and Technology (NIST). It is a contribution of the U. S. government, not subject to copyright.

Figure Captions

FIG. 1. Reciprocal images and real-space figures of the growth sequence for the epitaxial-Re/epitaxial-Al_2O_3/polycrystal-Al film. Refer to Ref. 30 for growth details. Under each k-space RHEED image we show a corresponding real-space figure depicting crystal ordering. (a) Epitaxial Re grown at 850 °C on a sapphire (0001) substrate. The streaks in the RHEED image indicate that the Re film is single-crystalline. (b) Amorphous AlO_x tunnel barrier reactively evaporated onto the base Re film at room temperature. Absence of a diffraction pattern implies that the as-grown AlO_x layer is amorphous. (c) Epitaxial Al_2O_3 formed after 800 °C annealing of the amorphous AlO_x. The streaks in the RHEED imply that the amorphous structure of (b) has transformed into a single-crystal. (d) Polycrystalline Al top electrode evaporated onto the epitaxial Al_2O_3 tunnel barrier. The multiple diffraction rings indicate that the top Al electrode is polycrystalline.

FIG. 2. Optical and schematic views of the epitaxial barrier qubit. (a) Optical micrograph of the fabricated qubit device. It is comprised of a qubit junction (70 μm^2 in area) on a quadrupole loop, a DC-SQUID and a flux bias coil. (b) Cross-sectional view of the qubit showing all the component layers; Al^1 (Al^2) stands for the UHV *in situ* evaporated (*ex situ* sputtered) aluminum. The amorphous SiO_2 (a-SiO_2) is used as an insulator between metallic wiring layers. (c) Schematic of the qubit and the measurement setup. For simplicity, some components such as filters are not shown here. On-chip components, which are cooled to 25 mK, are enclosed in a dotted box. The circuit parameters are $I_0 \approx$ 10 μA, $C \approx 2$ pF, $L \approx 115$ pH, $M \approx 1.1$ pH, and $M_S \approx 6.7$ pH.

FIG. 3. Qubit spectroscopy: probability of the qubit being in the $|1\rangle$ state after a long microwave ($f_{\mu w} \equiv \omega_{\mu w}/2\pi$) pulse is applied at each bias current; the brighter the color, the

higher the probability. When the microwave energy ($\hbar\omega_{\mu w}$) is equal to the energy spacing between the lowest two levels of the qubit ($\hbar\omega_{10}$), this probability reaches a maximum. (a) an amorphous barrier qubit (polycrystal-Al/amorphous-AlO_x/polycrystal-Al) and (b) an epitaxial barrier qubit (epitaxial-Re/epitaxial-Al_2O_3/polycrystal-Al). Both qubits have an identical design (qubit junction area of 70 μm^2) and the only difference is the trilayer structure. As reported previously, the amorphous barrier qubit (a) shows many spectral splittings. Each splitting can be seen more clearly in the zoomed-in image at the bottom inset. This situation is dramatically changed in the epitaxial barrier qubit (b). In (b), the density of splittings is substantially lower than that in (a). The bottom inset is a zoomed-in image of the spectrum. The top inset of (b) shows typical Rabi oscillation data of this epitaxial qubit measured at a bias point away from any splittings. Its exponentially fitted decay time is ~90 ns.

Figure 1

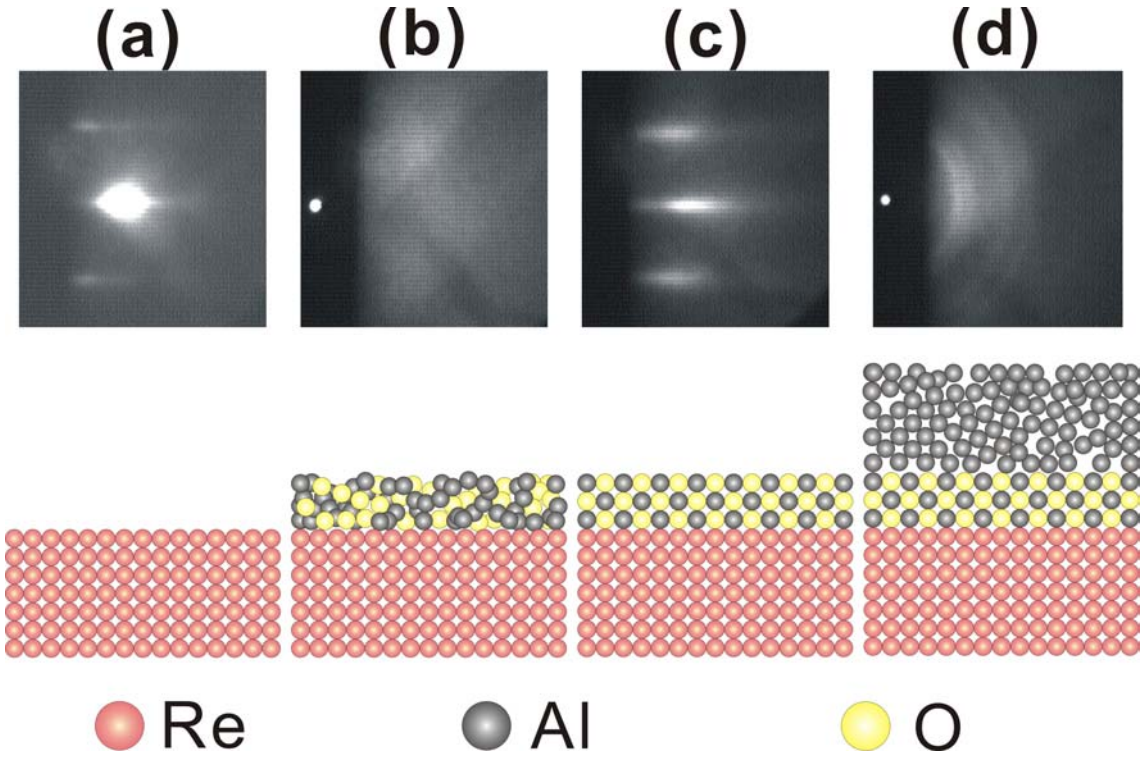

Figure 2

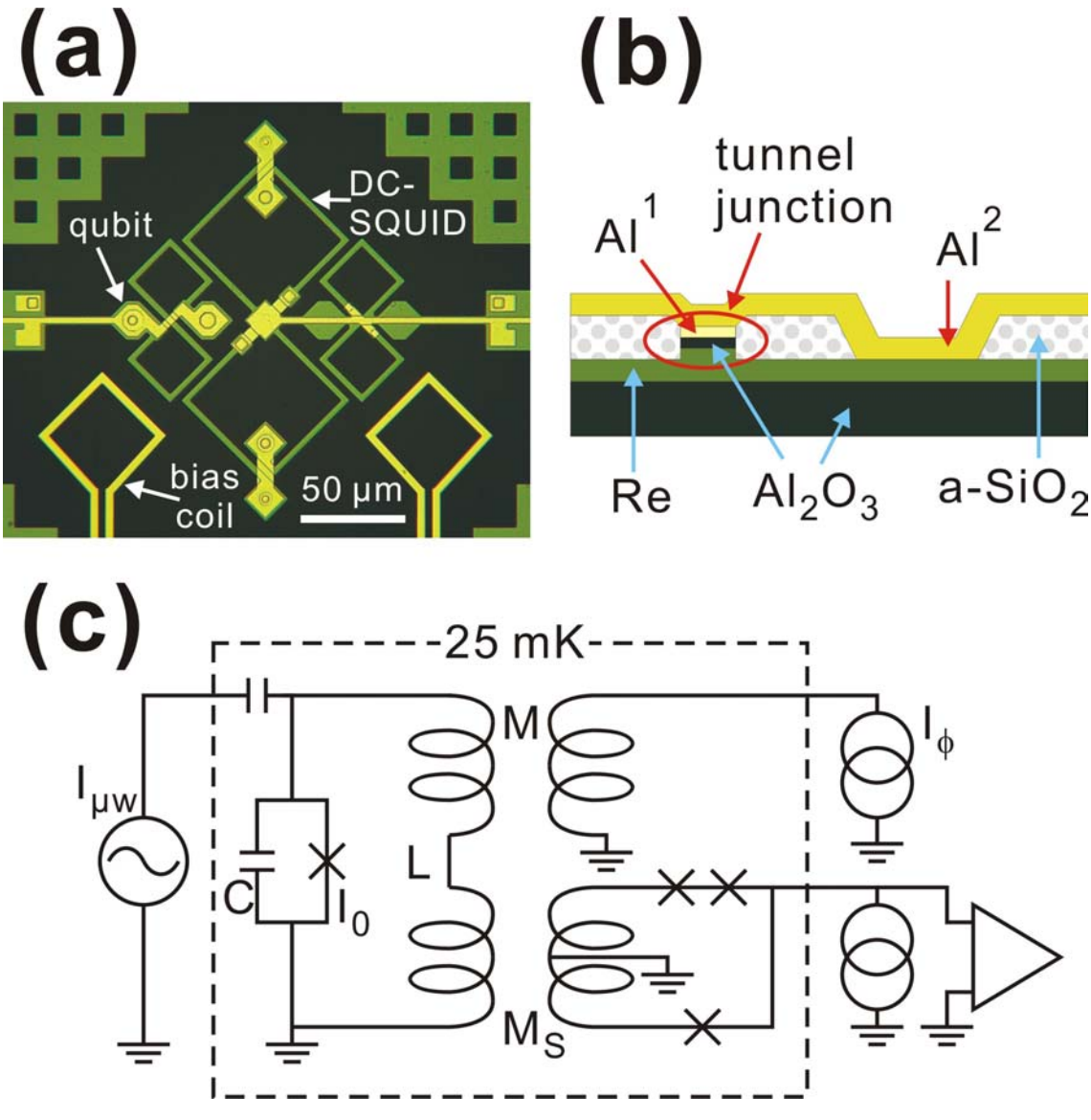
(a)
qubit
DC-
SQUID
bias
coil
50 μm
(b)
tunnel
junction
Al 1
Al 2
Re
Al2O3
a-SiO2
(c)
25 mK
Iμw
C
I0
L
M
MS
Iϕ

Figure 3

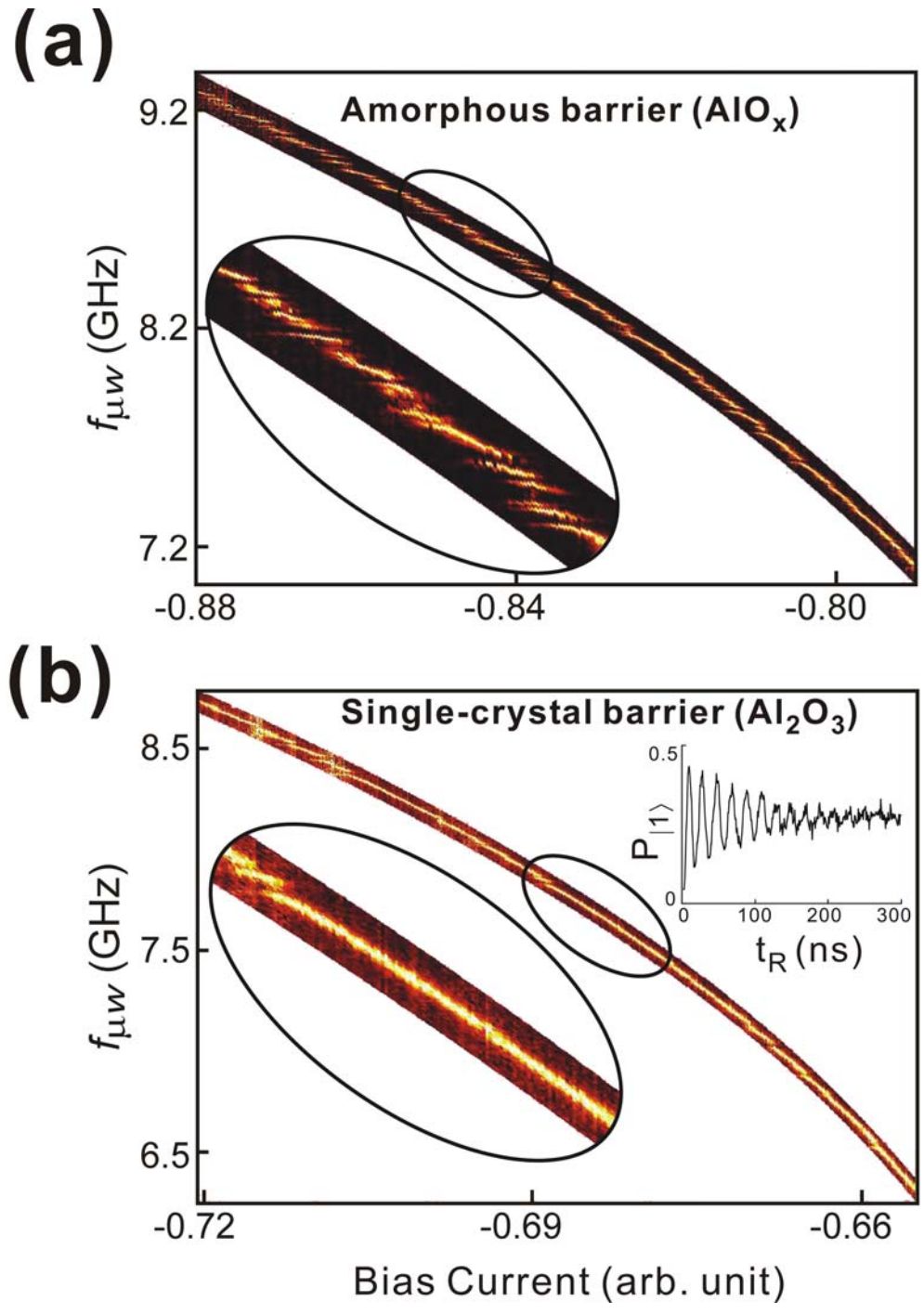
(a)
Amorphous barrier (AlO_x)
9.2
8.2
7.2
$f_{\mu w}$ (GHz)
-0.88
-0.84
-0.80
(b)
Single-crystal barrier (Al_2O_3)
8.5
7.5
6.5
$f_{\mu w}$ (GHz)
0.5
0
$P_{|1\rangle}$
0
100
200
300
t_R (ns)
-0.72
-0.69
-0.66
Bias Current (arb. unit)

References

[1] Y. Makhlin, G. Schön, and A. Shnirman, Rev. Mod. Phys. **73**, 357 (2001).

[2] Y. Nakamura, Yu. A. Pashkin, and J. S. Tsai, Nature **398**, 786 (1999).

[3] D. Vion, A. Aassime, A. Cottet, P. Joyez, H. Pothier, C. Urbina, D. Esteve, and M. H. Devoret, Science **296**, 886 (2002).

[4] J. M. Martinis, S. Nam, J. Aumentado, and C. Urbina, Phys. Rev. Lett. **89**, 117901 (2002).

[5] Y. Yu, S. Han, X. Chu, S.-I. Chu, and Z. Wang, Science **296**, 889 (2002).

[6] I. Chiorescu, Y. Nakamura, C. J. P. M. Harmans, and J. E. Mooij, Science **299**, 1869 (2003).

[7] Yu. A. Pashkin, T. Yamamoto, O. Astafiev, Y. Nakamura, D. V. Averin, and J. S. Tsai, Nature **421**, 823 (2003).

[8] A. J. Berkley, H. Xu, R. C. Ramos, M. A. Gubrud, F. W. Strauch, P. R. Johnson, J. R. Anderson, A. J. Dragt, C. J. Lobb, and F. C. Wellstood, Science **300**, 1548 (2003).

[9] J. B. Majer, F. G. Paauw, A. C. J. ter Haar, C. J. P. M. Harmans, and J. E. Mooij, Phys. Rev. Lett. **94**, 090501 (2005).

[10] R. McDermott, R. W. Simmonds, M. Steffen, K. B. Cooper, K. Cicak, K. D. Osborn, S. Oh, D. P. Pappas, and J. M. Martinis, Science **307**, 1299 (2005).

[11] T. Yamamoto, Yu. A. Pashkin, O. Astafiev, Y. Nakamura, and J. S. Tsai, Nature **425**, 941 (2003).

[12] I. Chiorescu, P. Beret, K. Semba, Y. Nakamura, C. J. P. M. Harmans, and J. E. Mooij, Nature **431**, 159 (2004).

[13] A. Wallraff, D. I. Schuster, A. Blais, L. Frunzio, R.-S. Huang, J. Majer, S. Kumar, S. M. Girvin, and R. J. Schoelkopf, Nature **431**, 162 (2004).

[14] L. M. K. Vandersypen, M. Steffen, G. Breyta, C. S. Yannoni, M. H. Sherwood, and I. L. Chuang, Nature **414**, 883 (2001).

[15] S. Gulde, M. Riebe, G. P. T. Lancaster, C. Becher, J. Eschner, H. Häffner, F. Schmidt-Kaler, I. L. Chuang, and R. Blatt, Nature **421**, 48 (2003).

[16] J. M. Martinis, M. H. Devoret, and J. Clarke, Phys. Rev. B **35**, 4682 (1987).

[17] P. Bertet, I. Chiorescu, G. Burkard, K. Semba, C. J. P. M. Harmans, D. P. DiVincenzo, and J. E. Mooij, Phys. Rev. Lett. **95**, 257002 (2005).

[18] Y. Nakamura, Yu. A. Pashkin, T. Yamamoto, and J. S. Tsai, Phys. Rev.Lett. **88**, 047901 (2002).

[19] R. W. Simmonds, K. M. Lang, D. A. Hite, S. Nam, D. P. Pappas, and J. M. Martinis, Phys. Rev. Lett. **93**, 077003 (2004).

[20] K. B. Cooper, M. Steffen, R. McDermott, R. W. Simmonds, S. Oh, D. A. Hite, D. P. Pappas, and J. M. Martinis, Phys. Rev. Lett. **93**, 180401 (2004).

[21] J. M. Martinis, K. B. Cooper, R. McDermott, M. Steffen, M. Ansmann, K. D. Osborn, K. Cicak, S. Oh, D. P. Pappas, R. W. Simmonds, C. C. Yu, Phys. Rev. Lett. **95**, 210503 (2005).

[22] L. Faoro and L. B. Ioffe, Phys. Rev. Lett. **96**, 047001 (2006).

[23] W. A. Phillips, Rep. Prog. Phys. **50**, 1657 (1987).

[24] A. Shnirman, G. Schön, I. Martin, and Y. Makhlin, Phys. Rev. Lett. **94**, 127002 (2005).

[25] L.-C. Ku and C. C. Yu, Phys. Rev. B **72**, 024526 (2005).

[26] D. J. Van Harlingen, T. L. Robertson, B. L. T. Plourde, P. A. Reichardt, T. A. Crane, and J. Clarke, Phys. Rev. B **70**, 064517 (2004).

[27] F. C. Wellstood, C. Urbina, and J. Clarke, Appl. Phys. Lett. **85**, 5296 (2004).

[28] I. Giaever, Phys. Rev. Lett. **5**, 147 (1960).

[29] A. I. Braginski, J. Talvacchio, M. A. Janocko, and J. R. Gavaler, J. Appl. Phys. **60**, 2058 (1986).

[30] S. Oh, K. Cicak, R. McDermott, K. B. Cooper, K. D. Osborn, R. W. Simmonds, M. Steffen, J. M. Martinis and D. P. Pappas, Supercond. Sci. Tech. **18**, 1396 (2005).

[31] W. E. Lee and K. P. D. Lagerlof, J. of Electron Microscopy Technique **2**, 247 (1985).